ChemComm

Bulk and Surface Structural Changes in High Nickel Cathodes Subjected to Fast Charging Conditions

Journal:	*ChemComm*
Manuscript ID	CC-COM-04-2020-002579
Article Type:	Communication

COMMUNICATION

Bulk and Surface Structural Changes in High Nickel Cathodes Subjected to Fast Charging Conditions

Received 00th January 20xx,
Accepted 00th January 20xx

DOI: 10.1039/x0xx00000x

Tianyi Liu,[a,b] Zhijia Du,[a,*] Xianyang Wu,[a,c] Muhammad M. Rahman,[b] Dennis Nordlund,[d] Kejie Zhao,[c] Michael D. Schulz,[b] Feng Lin,[b] David L. Wood, III,[a,e] Ilias Belharouak [a,e,*]

Layered oxide cathode, LiNi0.6Mn0.2Co0.2O2, undergoes sensible crystal expansion by losing significantly higher amounts of Li^+ at the end of fast charging cycles. However, the bulk structure of the cycled NMC622 is restored back to its pristine discharged state when intercalated with enough lithium ions during an electrochemically designed process.

Li-ion batteries (LIBs) are making steady inroads into electric vehicles (EVs).[1] However, the value proposition of electric cars is challenged by several hurdles including cost, safety and higher charging times in comparison with internal combustion engine vehicles (ICEs).[2,3] EVs typically require over 60 minutes to get 80 % state of charge (SOC) while an ICEs can be refueled in less than 5 minutes. Therefore, developing Li-ion batteries with extreme fast charging (XFC) capability is becoming a requisite to improve both public acceptance and market penetration of EVs. Here, the time required to realize XFC is defined as 10 min charging of the battery (6C-rate) to reach 80 % state of charge. Under such conditions, cell capacity decay is found to be extremely fast in most battery systems.[4,5] And, the research community has been investigating the underlying reasons for the degradation of materials performance. Of peculiar interest, three major reasons have been reported, (1) lithium plating on graphite anodes, (2) dissolution of transition metals in layered oxide cathodes , and (3) reduction of lithium inventory in cathodes.[4,5] Most of these reports mainly focus on electrochemical performance deterioration rather than on acquiring chemical and structural changes of each individual cell component upon completion of fast charging cycles.

Layered structure oxides containing nickel, manganese and cobalt ($LiNi_xMn_yCo_zO_2$, labeled NMCXYZ, x+y+z = 1) are the most promising cathode candidates for next generations of Li-ion batteries,[6-7] where Ni is responsible for the high specific capacity while Mn and Co ensure structural and thermal stability.[8-9] Cathode material $LiNi_{0.6}Mn_{0.2}Co_{0.2}O_2$, NMC622 in particular, has balanced advantages in terms of energy density, cost and thermal stability and performance under non extreme fast charging conditions.[10,11]

Here, we report the cycling performance of $LiNi_{0.6}Mn_{0.2}Co_{0.2}O_2$/graphite cells under different charging rates are shown in Fig. 1a. The capacity retention of the cells after 200 cycles significantly dependent on the charging rates. Indeed, the capacity retention was 90% under the 1C/1C charge/discharge, while it was only 50% under the 6C/1C charge/discharge. Fig. 1b compares the voltage profiles of the NMC622/graphite cells. During the 6C charging, the cell reached the cut-off voltage, 4.2 V, in less than 10 minutes. Then, we added a constant voltage hold at 4.2 V to the charging profile to finish 10 min total charging time, which accounted for an increased portion of the total capacity as cycling continued. After 10 cycles, more than 50% of the charging capacity was from the constant voltage holds. Differential capacity (dq/dv) analyses are shown in Fig. 1c and d. Under a low rate (C/3), there are two major redox peaks during charge, corresponding to Li^+ intercalation into graphite and its simultaneous de-intercalation from the cathode.[12,13] These two peaks merged into a one peak when the cells were charged and discharged at the 1C rate, and their shapes were quite identical on cycling. However, the scenario became significantly different as the redox peaks almost vanished when the cells were charged and discharged at the 6C/1C, respectively (Fig.1d). This phenomenon is attributed to the higher polarization from the six-fold higher current used to attain fast charging.

[a] *Energy and Transportation Science Division, Oak Ridge National Laboratory, Oak Ridge, TN 37830, USA. Email: duz1@ornl.gov. Tel.: 1-(865)574-7519.*
[b] *Department of Chemistry, Virginia Tech, Blacksburg, VA 24061, USA.*
[c] *School of Mechanical Engineering, Purdue University, West Lafayette, IN 47907, USA.*
[d] *Stanford Synchrotron Radiation Lightsource, SLAC National Accelerator Laboratory, Menlo Park, CA 94025, USA.*
[e] *Bredesen Center for Interdisciplinary Research and Graduate Education, University of Tennessee, Knoxville, TN 37996, USA. Email: belharouaki@ornl.gov*
† Electronic supplementary information (ESI) available. See DOI: 10.1039/x0xx00000x

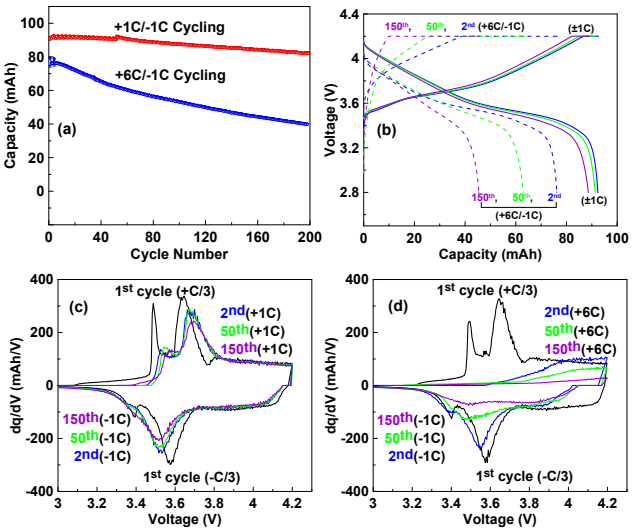

Fig. 1. Electrochemical performance of NMC 622/graphite cells under different C-rates. (a) cycling performance of batteries; (b) voltage profiles; (c) dq/dV curves obtained under 1C/1C rate (d) dq/dV curves obtained under 6C/1C.

Fig. 2 shows the results obtained by synchrotron x-ray diffraction in order to study the bulk structural changes of NMC622. The samples were recovered from cells discharged to 1.0 V. The hexagonal layered structure of the NMC622 cathode is well maintained upon completion of fast charge cycles and can be indexed to $R\bar{3}m$ [166] space group. However, we observed peak shifts and intensity changes in a closer examination. Fig. 2b shows that the (003) diffraction line shifts to lower angles after repeated 6C/1C cycling, which indicates an expansion of the hexagonal unit cell along the c-direction (Fig. 2b). This expansion is correlated with the loss of Li^+ in NMC622. Indeed, with less Li-ions in the transition metal slabs, the repulsive forces between O^{2-} anions become stronger. We also observed a larger separation between the diffraction lines (108) and (110) (Fig. 2c), which further substantiates our hypothesis on the loss of lithium inventory in the cathode.[14] Units cell parameters obtained by Rietveld refinement are shown in Fig. 2d (see Fig. S1 also). The interlayer distance between two transition metal layers (c parameter) increased from ~14.26 Å to ~14.37 Å after repeated fast charging cycles. Moreover, the increasing intensity ratio of the (003)/(104) peaks (Fig. 2b) is an indication of a lower degree of cation mixing in the lattice, which suggests that the average oxidation state of Ni is higher owing to the higher Li^+ amounts that were lost from the cathode during fast charging.[15] Anti sites occur in $LiNi_xMn_yCo_zO_2$ cathodes with higher nickel content (>50%) because the radius of Ni^{2+} is closer to that of Li^+. With the vanished Li^+ on cycling, it is likely that the crystalline structure of NMC622 shows less disorder between the lithium and transition metal slabs. It is worth noting that the Li^+ inventory lost in NMC622 is gained by graphite via the continuous growth of SEI and/or lithium plating on the anode side (Fig. S2).

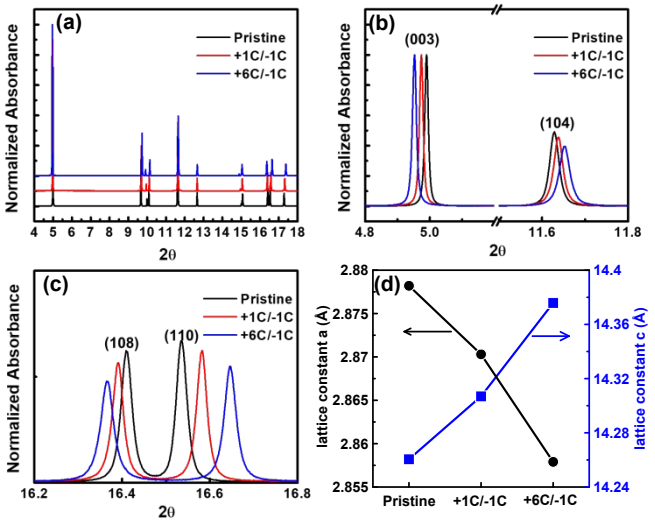

Fig. 2. (a) Synchrotron XRD patterns for NMC622 cathode after 200 cycles. Wavelength = 0.412798 Å. (b) detailed (003) and (104) peaks. (c) separation of (108) and (110) peaks. (d) Rietveld refinement results on the lattice constant a and c.

X-ray absorption near edge spectroscopy (XANES) results are shown in Fig. 3a to discuss the chemical and local environment of nickel in the bulk of NMC622.[16] Indeed, the oxidation state and chemical environment of Ni reflect the chemical change of the material because the charge compensation is mainly achieved by Ni redox in NMC materials.[17] The magnified Ni K-edge, presented in Fig. 3b, shows that the Ni K-edge energy position of the 1C/1C cycled material overlaps with the pristine. However, the Ni K-edge clearly shifted to higher energies under the 6C/1C rate condition, indicating a higher average oxidation state of Ni upon fast charging cycles. This observation is also consistent with the higher Li^+ loss as revealed by the XRD result discussed above. The magnification of the Ni pre-edge is shown in Fig. 3c. The pre-edge peak of NMC622 from the 6C/1C cycled cell has a broader shape than the ones from 1C/1C cycled cell and pristine material. The peak also shifts to a higher energy position, which is associated with the slight distortion of the octahedral site or the chemical environment change.[18,19] Surface information at a depth of 5-10 nm is depicted by the soft XAS results shown in Fig. 3d. The oxidation state of Ni at the surface of the cathode is reflected by the intensity ratio of peak B/A, i.e. the higher is the peak ratio the higher is oxidization state of Ni.[10,20] The Ni at the surface of NMC622 from the 6C/1C cycled cell is more reduced than the one from 1C/1C cycled cell. Surface reduction phenomenon is commonly found in several high-nickel content cathodes due to their surface reconstruction and instability of $Ni^{3+/4+}$.[10,20] This opposite behavior in oxidation states of nickel reveals that the bulk and surface of high nickel cathodes have antagonistic responses to fast charging conditions.

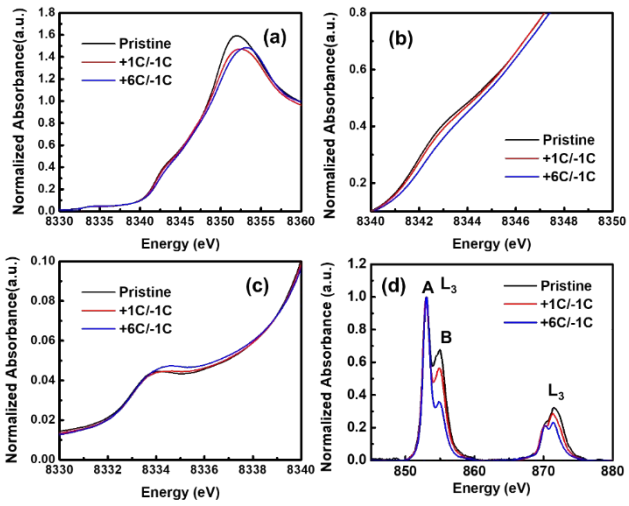

Fig. 3. (a) Hard XAS of Ni K-edge for pristine NMC622 cathode and after 200 cycles under 1C/1C and 6C/1C charge/discharge rates. (b) A magnification of the Ni- K edge in (a). (c) A magnification of the Ni pre-edge in (a). (d) Soft XAS of Ni L-edge for pristine NMC622 cathode and after 200 cycles under 1C/1C and 6C/1C charge/discharge rates.

Coin cells were made using the cycled NMC622 cathode, Li metal and fresh electrolyte to test the reversibility of the spent cathodes. Fig. 4 shows the charge and discharge voltage profiles of these spent cathodes in comparison with pristine NMC622. During the first charge, the specific capacity of the spent NMC622 cathode recovered from the 6C/1C cycled cell was 105 mAh/g in comparison to 138 mAh/g for the 1C/1C cycled cell. This 105 mAh/g capacity, in comparison with the full capacity of 168 mAh/g, demonstrates that $LiNi_{0.6}Mn_{0.2}Co_{0.2}O_2$ lost about 37% of lithium during the fast charging cycles. During the first discharge, the cathode NMC622 recovered from the 6C/1C cycled cell regained about 95% of its initial specific capacity. The 5% capacity difference could be due to (1) particles cracking and loss of contact between particles,[21] (2) possible dissolution of transition metal on cycling,[22] and (3) reconstruction of surface cathode as discussed above. From the structural standpoint, the high level of capacity recovery suggests that the NMC622 cathode can restore most of lithium inventory despite its extensive cycling under high rate charge conditions. This result is very consistent with the XRD and XAS results that confirm that the layered structure of NMC622 is robust enough under fast charging rates.

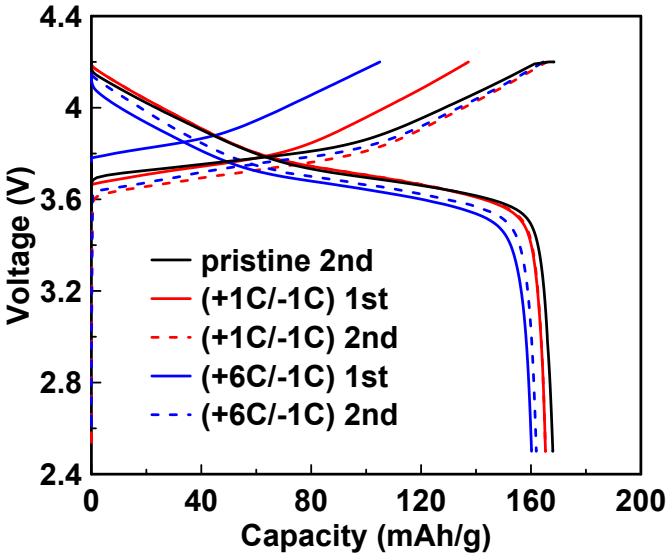

Fig. 4. Voltage curves of Li cells assembled with NMC622 cathode after 200 cycles under 1C/1C and 6C/1C charge/discharge rates. The material was delithiated and lithiated at a constant rate of C/10 between 2.5 and 4.2 V.

In summary, the surface and bulk changes of $LiNi_{0.}6Mn_{0.2}Co_{0.2}O_2$ has been studied upon completion of extensive cycling under fast charging cycles. XRD results revealed that the material lost significant amount of Li^+ which resulted in higher "c" lattice parameter and volume expansion. XANES results proved that the bulk oxidation state of Ni in the 6C-rate charged NMC622 is higher than both the pristine and 1C-rate charged cathodes. Soft XAS results revealed, however, that the oxidation state of Ni is lower at the cathode surface and that a possible surface reconstruction occurred during fast charging cycles. Despite the extreme fast charging condition, NMC622 structure remains prone to intercalating most of the 35% lithium inventory lost when assembled in lithium cells. This study provides new insights on the reasons behind the capacity fade in fast charged cells, and those can be summarized in (1) loss of Li-ion inventory in cathodes, (2) heavy Li plating on graphite and (3) cathode cracking and surface reconstruction.

This research at Oak Ridge National Laboratory, managed by UT Battelle, LLC, for the U.S. Department of Energy (DOE) under contract DE-AC05-00OR22725, was sponsored by the Office of Energy Efficiency and Renewable Energy (EERE) Vehicle Technologies Office (VTO) (Technology Manager: Brian Cunningham). This research used resources of the Advanced Photon Source, a U.S. Department of Energy (DOE) Office of Science User Facility operated for the DOE Office of Science by Argonne National Laboratory under Contract No. DE-AC02-06CH11357. Use of the Stanford Synchrotron Radiation Lightsource, SLAC National Accelerator Laboratory, is supported by the U.S. Department of Energy, Office of Science, Office of Basic Energy Sciences under Contract No. DE-AC02-76SF00515.

Conflicts of interest

There are no conflicts to declare.

Notes and references

1 N. Lutsey, *Int. Counc. Clean Transp.*, 2015, **2015**, 5.
2 L. Lu, X. Han, J. Li, J. Hua and M. Ouyang, *J. Power Sources*, 2013, **226**, 272–288.
3 S. B. Peterson, J. Apt and J. F. Whitacre, *J. Power Sources*, 2010, **195**, 2385–2392.
4 C. Mao, R. E. Ruther, J. Li, Z. Du and I. Belharouak, *Electrochem. commun.*, 2018, **97**, 37–41.
5 T. R. Tanim, E. J. Dufek, M. Evans, C. Dickerson, A. N. Jansen, B. J. Polzin, A. R. Dunlop, S. E. Trask, R. Jackman, I. Bloom, Z. Yang and E. Lee, *J. Electrochem. Soc.*, 2019, **166**, A1926–A1938.
6 A. Manthiram, 2017, 1063–1069.
7 P. Kalyani and N. Kalaiselvi, *Sci. Technol. Adv. Mater.*, 2005, **6**, 689–703.
8 M. S. Whittingham, Y. S. Meng, J. Bréger, C. P. Grey and G. Ceder, *Science*, 1976, **192**, 1126–7.
9 M. Yoshio, H. Noguchi, J. Itoh, M. Okada and T. Mouri, *J. Power Sources*, 2000, **90**, 176–181.
10 C. Tian, D. Nordlund, H. L. Xin, Y. Xu, Y. Liu, D. Sokaras, F. Lin and M. M. Doeff, *J. Electrochem. Soc.*, 2018, **165**, A696–A704.
11 C. Tian, Y. Xu, D. Nordlund, F. Lin, J. Liu, Z. Sun, Y. Liu and M. Doeff, *Joule*, 2018, **2**, 464–477.
12 R. Jung, M. Metzger, F. Maglia, C. Stinner and H. A. Gasteiger, *J. Electrochem. Soc.*, 2017, **164**, A1361–A1377.
13 H.-J. Noh, S. Youn, C. S. Yoon and Y.-K. Sun, *J. Power Sources*, 2013, **233**, 121–130.
14 Ilias Belharouak, Wenquan Lu, Donald Vissers and Khalil Amine, *Electrochem. commun.*, 8, 329–335.
15 J. Zhao, W. Zhang, A. Huq, S. T. Misture, B. Zhang, S. Guo, L. Wu, Y. Zhu, Z. Chen, K. Amine, F. Pan, J. Bai and F. Wang, *Adv. Energy Mater.*, 2017, **7**, 1601266.
16 M. G. K. and and C. H. Yo*, , DOI:10.1021/JP990753B.
17 T. Ohzuku and Y. Makimura, *Chem. Lett.*, 2001, **30**, 642–643.
18 F. de Groot, G. Vankó and P. Glatzel, *J. Phys. Condens. Matter*, 2009, **21**, 104207.
19 Y. W. Tsai, B. J. Hwang, G. Ceder, H. S. Sheu, D. G. Liu and J. F. Lee, *Chem. Mater.*, 2005, **17**, 3191–3199.
20 F. Lin, I. M. Markus, D. Nordlund, T. C. Weng, M. D. Asta, H. L. Xin and M. M. Doeff, *Nat. Commun.*, 2014, **5**, 3529.
21 Y. Mao, X. Wang, S. Xia, K. Zhang, C. Wei, S. Bak, Z. Shadike, X. Liu, Y. Yang, R. Xu, P. Pianetta, S. Ermon, E. Stavitski, K. Zhao, Z. Xu, F. Lin, X. Q. Yang, E. Hu and Y. Liu, *Adv. Funct. Mater.*, , DOI:10.1002/adfm.201900247.
22 R. Jung, F. Linsenmann, R. Thomas, J. Wandt, S. Solchenbach, F. Maglia, C. Stinner, M. Tromp and H. A. Gasteiger, *J. Electrochem. Soc.*, 2019, **166**, A378–A389.